

Original Research Article

INNOVATIVE WIND ENERGY GENERATING DEVICE COUPLED WITH AIR CONVERGENT

ABSTRACT:

Aims: Researchers are more and more focused on finding ways to optimize renewable energy sources. One of the more promising of these renewable energies is wind energy. However, these wind resources are very localized and selective. There is also significant potential for wind resources available at low densities or low wind speeds. The objective of this research is to exploit these resources.

Methodology: To do so, this study proposes a new wind generating device coupled with a flow convergent in order to increase its performance at low wind speed. This new wind device is designed under Solidworks and analyzed with Matlab software. Several parameters are simulated. The effect of the pulley transmission ratio on the mechanical values of the generator, the impact of the operating gas in terms of angular velocity, power and torque on the generator shaft was clearly determined.

Results: It appears that the power at the input of the wind device is multiplied by the square of the ratio of the output and input velocities, the flow passing through the convergent being constant. The torque on the generator decreases with the increase of the transmission ratio while its speed increases. However, for a fixed transmission ratio, the speed remains constant while the torque and power increase with the speed at the inlet of the convergent. On the other hand, it is noted that, the lower the adiabatic coefficient of the gas used, the higher the power generated.

Conclusion: When used with a wind device, the output parameters of the convergent will result in better mechanical efficiency, which greatly improves electrical power generation.

Keywords: wind energy, optimized output parameters, innovation design, torque and power.

NOMENCLATURE

\mathcal{P}_{theo} : theoretical power at the convergent input (*Watt*)
 $\mathcal{P}_{recoverable}$: Recoverable power at the convergent output (*Watt*)
 \dot{m}_{max} : maximum mass flow (*kg. h⁻¹*)
 U_{max} : maximum flow velocity (*m. s⁻¹*)
 F_{theo} : theoretical force on the blades (*N*)
 R : disc radius + arm length + blade diameter (*mm*)
 Ω_D : disc angular velocity (*rd. s⁻¹*)
 M_o : moment of F_{theo} (*N. m*)
 N_{GP} : large pulley rotation speed (*trs. min⁻¹*)
 N_{ax} : small pulley rotation speed (*trs. min⁻¹*)
 R_{GP} : large pulley radius (*mm*)
 R_{PP} : small pulley radius (*mm*)
 C_{ax} : torque on the axis of the generator (*N. m*)
 γ : adiabatic coefficient

1. INTRODUCTION:

The world's need for energy and electrical power continue to grow. As fossil fuel reserves are depleted, attention has shifted to renewable energy production to make human energy use and demand more sustainable. Several factors are driving this trend. Additionally, the unprecedented effects of climate change and global warming are driving a more rapid response. The energy of the future encompasses renewable energy resources for sustainable environmental protection and economic development. These are useful energies that renew themselves naturally, including solar energy, biomass, geothermal energy, hydro energy, and wind energy. Among these resources, wind has become one of the main energy opportunities for the massive production of electricity.

In most cases, wind turbines are primarily used to convert the kinetic energy of moving air into rotating mechanical energy that is converted into electrical energy by generators [1]. The energy produced by wind turbines generally depends on the geographical location, weather conditions and the type of turbine [2]. According to their configuration and orientation, they can be categorized as horizontal axis wind turbines (HAWT) or vertical axis wind turbines (VAWT) [3]. Several studies have compared these two types of wind turbines and highlighted the advantages and limitations of each type [4,5].

HAWTs allow for higher energy efficiency and therefore lower cost of energy produced, but this is only possible at high wind speeds. In addition, turbulence, variations, or excessive directional variability of the wind can cause significant problems in the use of HAWTs. On the other hand, VAWTs have demonstrated their ability to meet certain power generation requirements that cannot be met by HAWTs [5]. Despite the lower efficiency and variable output of VAWTs, various advantages of VAWTs that could outweigh their limitations are evidenced, especially under certain circumstances. Specifically, VAWTs are almost capable of harnessing wind in all directions, so they can operate regardless of the wind direction. In fact, these turbines do not require high wind speeds to produce energy. Therefore, they can be installed in locations with modest wind speeds and can be mounted close to the ground, which facilitates maintenance and control. On the other hand, since they generate lower forces on their supporting structure, their structural design is simpler, and they are less noisy [4]. Similarly, VAWTs can be a promising solution for power generation in remote locations away from integrated grids [6].

Basically, there are several design variants of wind devices depending on the operating principles, blade shape and configuration. A comprehensive review of these different types and their performance has been presented in [6, 7]. Thus, there are cross-flow wind turbines [8], with power augmentation devices such as the stator, guide vanes and nozzles [9], flow convergent [10], symmetrical box [11], has rows of guide vanes [12], omnidirectional guide vanes (ODGV) [13], wind booster [14].

Several scientific works have addressed the evaluation and improvement of wind turbine performance over the last two decades. The performance of different wind turbine designs and configurations as well as the effect of design parameters have been studied using various approaches. Other research teams have used field experiments to study the effect of certain wind variables such as wind speed, wind direction and turbulence intensity [15, 16]. In terms of improving the characteristics of wind turbines, various design modifications and optimizations as well as innovative design ideas have been investigated. The influence of blade shape parameters on self-starting and energy extraction efficiency has attracted scientists' attention [17–20]. However, others have focused on improving the performance by using composite blades [21, 22]. In addition, the effect of the number of blades used in some

turbines has also been studied [16]. Moreover, some researchers have focused on the use of different turbine blade configurations, such as the cross-axis turbine proposed in [23]. Still others have promoted the use of different wind guidance devices to improve the performance of the turbine, such as guide vans, windscreens, and baffles. A comprehensive review of these devices and their effect on self-starting ability as well as power generation has been provided in [24].

In this study, a flow convergent is mounted on a wind device to improve its output parameters. Several design variations including various convergent arrangements were also performed to investigate the effect of maximum power output. The optimal design of the blade disk and the flow convergent leads to a better configuration between the wind flow and the receiving face for continuous rotation and thus higher efficiency.

2. MATERIAL AND METHODS

The wind prototype, as well as its functioning, are outlined in this section. The various simulation parameters are presented.

2.1 Modeling

The solid model of the wind device prototype is designed in SolidWorks according to the desired output parameters. The following fig. 1 represents the different parts of the device, mounted in operating condition in the laboratory.

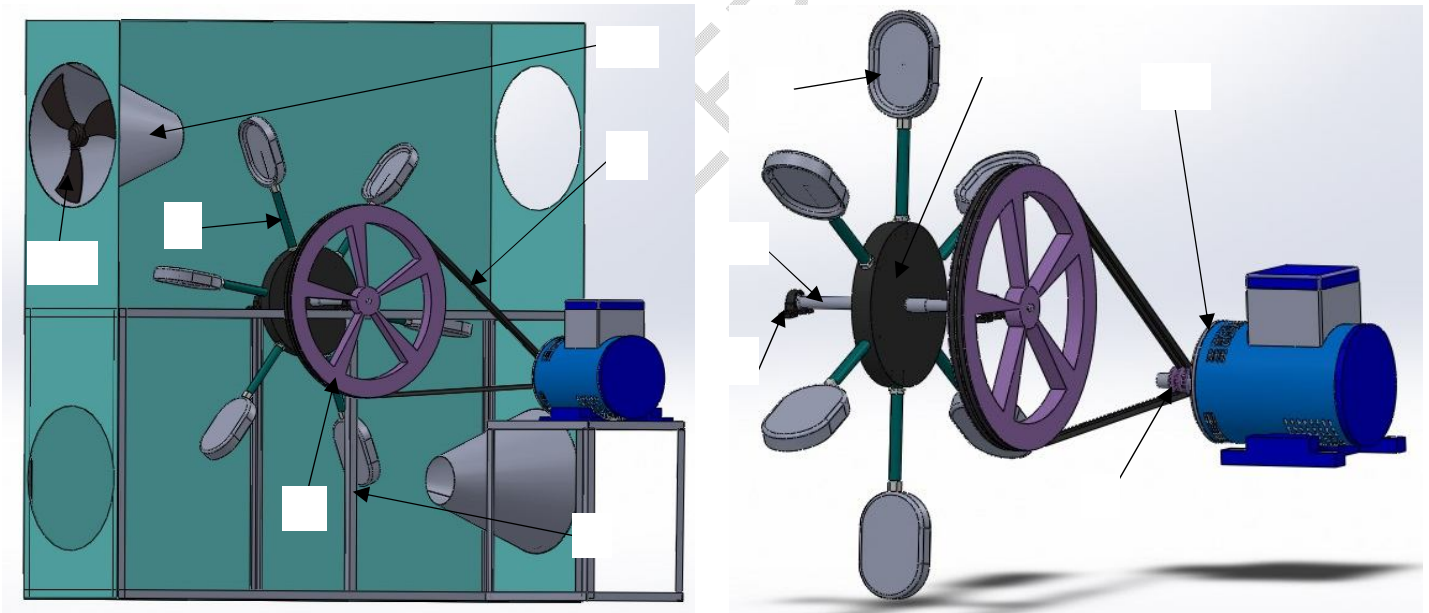


Fig. 1: Mechanical model of the convergent flow wind device

- 1- Support
- 2- (2) bearings
- 3- Shaft
- 4- Solid cylindrical disc
- 5- Torr iron arms
- 6- Sheet metal blades

- 7- Driven pulley attached to the axis of a motor
- 8- Driving pulley
- 9- Power transmission belt between pulleys
- 10- Generator
- 11- (2) Convergent
- 12- (2) fans delivering an airflow

A fan delivers an appropriate wind flow. In relation to the density of the air and the large cross-section of the convergent, this results in a wind speed that is brought to a given maximum, if the choice of the cross-sections of the convergent respects [10]. Assuming that the device generates losses that do not exceed those evaluated by Betz, the recoverable power has the following theoretical form:

$$\mathcal{P}_{theo} = 16/27 \cdot \mathcal{P}_{recoverable} = 8/27 \dot{m}_{max} U_{max}^2$$

The instantaneous effects of this power are a force exerted on the blade and a moment applied to the device given respectively by:

$$F_{theo} = \mathcal{P}_{theo}/U_{max} = 8/27 \dot{m}_{max} U_{max}$$

$$M_o = F_{theo} \cdot R$$

where R is the length (5), of the torr iron arm plus the radius of the disk, plus the diameter of a blade (4).

The shaft (3) of the device is thus driven in rotation in the bearings (2). The rotation of the shaft (3) leads the driving pulley (8) which transmits the power of the driven pulley (7) via the belt (9). In this way, the generator (10) is driven to produce electrical energy. Previously published research [10] has demonstrated the efficiency and wind speed multiplication that the convergent bring to the wind device. For selected sections, there is a multiplication of the order of more than 10 times the input speed at the exit of the convergent.

It should be mentioned that, except for the conditions of the generating state imposed by the fan, the only way to set a given power to the device, results from the choice of the section A^* of the collar or of the critical section. In practice, this section will be that of a blade. Once A^* is chosen, the cross-sectional area A can be calculated [10].

2.2 Torque and angular velocity on the generator shaft

The theoretical power is transmitted to the generator shaft as follows.
The angular velocity of the disc:

$$\Omega_D = \mathcal{P}_{theo}/M_o$$

The angular velocity of the disc and also of the large pulley is:

$$N_{LP} = \frac{30}{\pi} \Omega_D$$

The angular velocity on the generator shaft:

$$N_{ax} = \frac{R_{GP}}{R_{PP}} N_{GP}$$

The torque on the generator shaft:

$$C_{ax} = \frac{30}{\pi} \cdot \frac{\mathcal{P}_{theo}}{N_{ax}}$$

The power of the generator shaft:

$$\mathcal{P}_{ax} = \mathcal{P}_{theo}$$

2.3 Operating gas impact

It is remarkable that, from all the above, the quality of the operating gas (air), is crucial in the results obtained. Therefore, it becomes interesting to review the results obtained with regard to other gases available in nature that could, in one way or another, be substituted for air. The growing need for energy should not allow for any negligence whatsoever.

It is important, before going further in the investigations, to present a table of the thermodynamic parameters of some common gases.

Table 1: Values of some thermodynamic constants of several gases.

Gaz	Mass (kg/kmole)	C_p (J/kg/K)	C_v (J/kg/K)	r (J/kg/K)	γ
Air	28.97	1005	718	287.1	1.4
Water vapor (H_2O)	18.02	1867	1406	61.4	1.33
Methane (CH_4)	16.04	188.9	1687	518.7	1.32
Carbon dioxide (CO_2)	44.01	846	653	188.9	1.3
Ethylene (C_2H_4)	28.05	1548	1252	296.4	1.24
Acetylene (C_2H_2)	26.04	1712	1394	319.6	1.23
Ethane (C_2H_6)	30.07	1767	1495	276	1.18
Propane (C_3H_8)	44.09	1692	1507	188.3	1.12
Isobutane (C_4H_{10})	58.12	1758	1620	143.1	1.09
Octane (C_8H_{18})	114.23	1711	1638	72.8	1.04

2.4 Use of the device in an environment

For this case, the minimum wind speed at the site is expected and the wind direction will also be considered. With the choice of the convergent, it is simply necessary to adapt the device. It will be required however, to take care to place the opening of the convergent in the direction of the wind.

If, in order to ensure an unbiased operation of the device, it is decided to have two or three convergents, the device will be slightly modified to consider the wind direction. This would lead to the scheme below (Fig. 2).

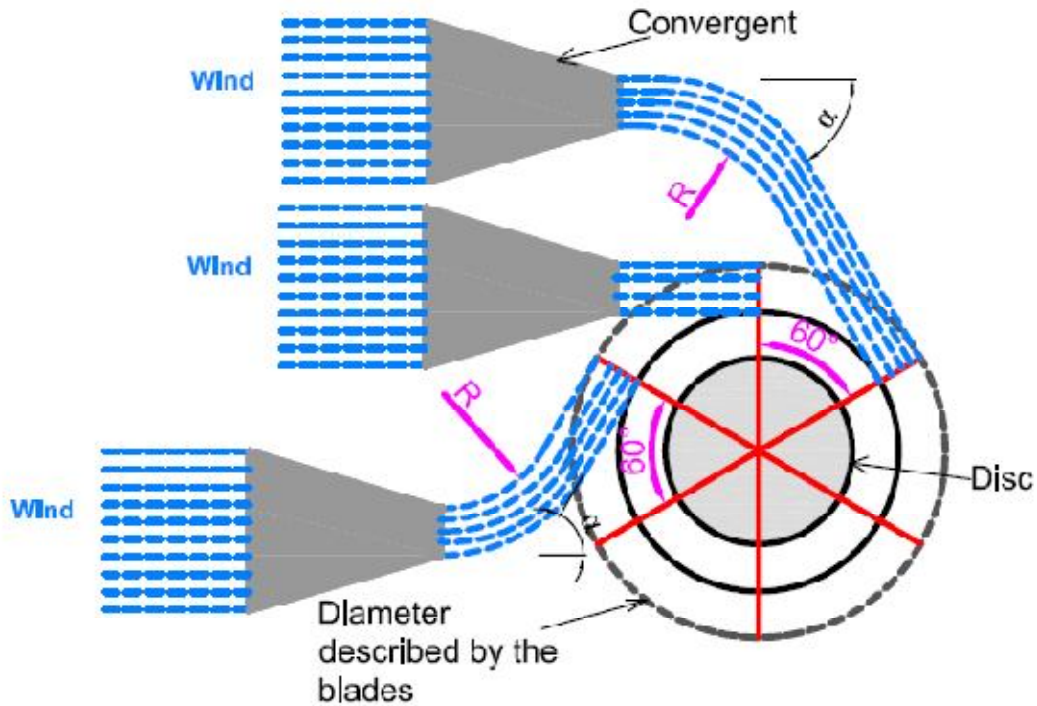


Fig. 2: Device with 3 convergents used in environment

The scheme in Fig. 2 is suitable for exposure at an appropriate site. It will be necessary, however, to make a proper calibration of the device. A power level must be installed in relation to the site's speed threshold to ensure a minimum energy supply.

2.5 Pressure losses in the bent convergent

Modifying the second convergent to fit the device is a matter of determining the proper radius of curvature that would minimize the pressure drop. Wiesbach's relationship for large opening round bends is intended as an expression of the singular pressure drop coefficient as a function of radius of curvature, angle, and outlet diameter. It is expressed as follows:

$$K = \frac{\alpha}{\pi} \left[0.131 + 1.847 \left(\frac{D}{R} \right)^{7/2} \right]$$

It is established for some operating conditions and from a Matlab program the figures below:

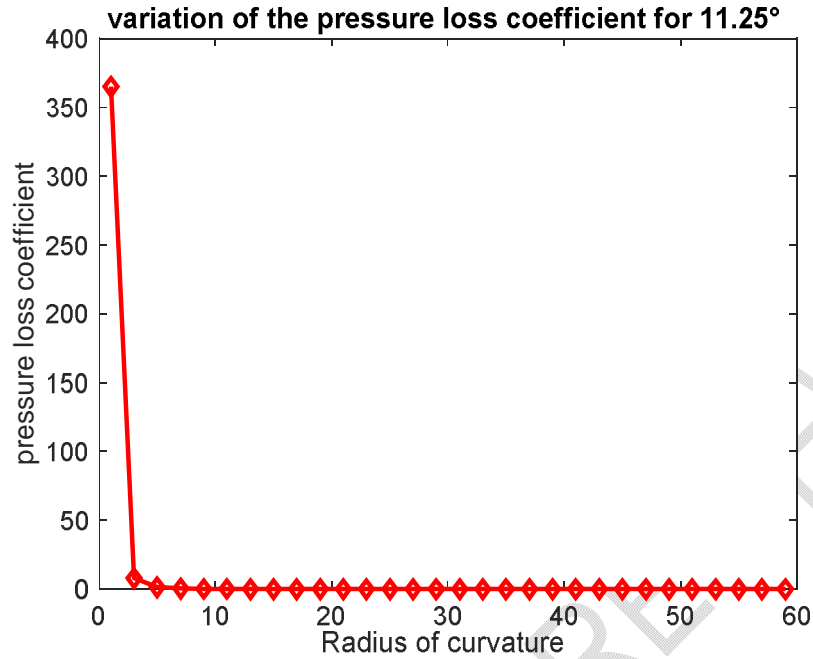


Fig. 3: Variation of the pressure loss coefficient for $\alpha = 11.25^\circ$

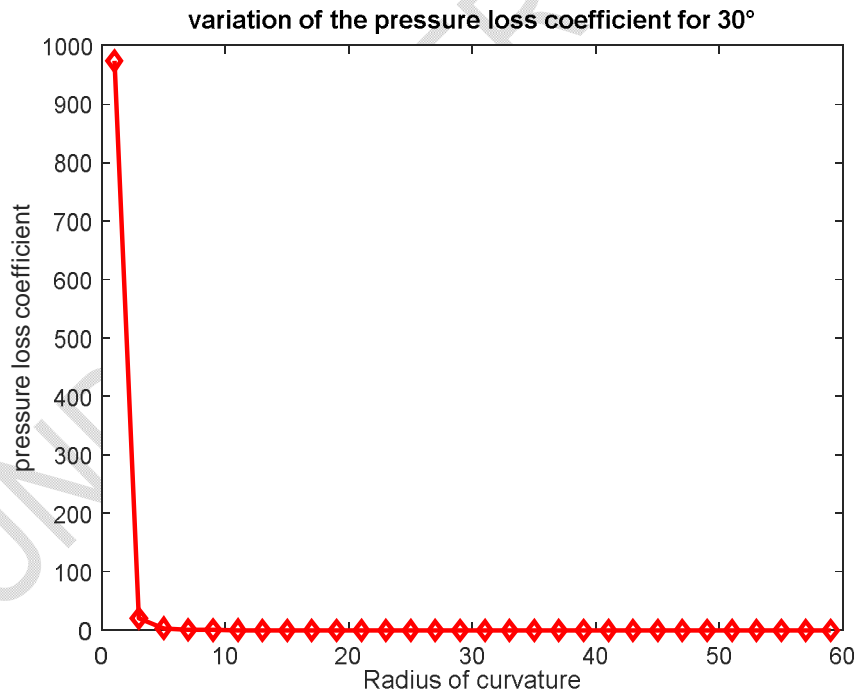


Fig. 4: Variation of the pressure loss coefficient for $\alpha = 30^\circ$

From Fig. 3 and Fig. 4, it can be simply found the minimum pressure loss coefficient for the cases studied. These values are reported in the table 2 and table 3 for different value of α .

Table 2: Radius of curvature and pressure loss coefficient values for $\alpha = 11.25^\circ$

Angle 11.25° or $\pi/16$											
R	13	15	17	19	21	23	25	27	29	31	33
K	0.05 43	0.03 61	0.02 62	0.02 04	0.01 68	0.01 44	0.01 29	0.01 18	0.01 10	0.01 04	0.01 00

Table 3: Radius of curvature and pressure loss coefficient values for $\alpha = 30^\circ$

Angle 30° or $\pi/6$											
R	13	15	17	19	21	23	25	27	29	31	33
K	0.14 47	0.09 63	0.06 99	0.05 44	0.04 48	0.03 85	0.03 43	0.03 14	0.02 92	0.02 77	0.02 65

It can be noticed that for a fixed radius of curvature, the pressure loss coefficient increases with the angle. Similarly, for a fixed angle, the pressure loss coefficient decreases as the radius of curvature increases.

The choice of a configuration depends on economic, technical and technological constraints, but especially on the desired level of pressure drop.

With this configuration of convergents, one can estimate the overall power that the device provides at the output. Knowing that the right convergent delivers a power \mathcal{P}_{theo} , the bent convergents will deliver a power $(1 - K)\mathcal{P}_{theo}$. The global power of the device at the output will be:

$$\mathcal{P}_{glob} = (3 - 2K)\mathcal{P}_{theo}$$

The gain obtained in this device is mainly acquired at the convergent where the ratio of output and input powers is given by the expression:

$$\frac{\mathcal{P}_{theo_outlet}}{\mathcal{P}_{theo_inlet}} = \left(\frac{U^*}{U_0}\right)^2$$

with U^* and U_0 the velocities at respectively the outlet and the inlet of the convergent.

This equation above is justified by the fact that the flow rate remains constant in the convergent as soon as the threshold of the critical point is not crossed [10]. Indeed, beyond this point, shock waves appear, and important discontinuities are observed in the distribution of the flow parameters.

3. RESULTS AND DISCUSSION

An advanced Matlab program was used to produce the mechanical values of the generator. Taking for air, ($\gamma=1.4$) and setting ($U_0=4 \text{ ms}^{-1}$), the following curves are drawn in Excel.

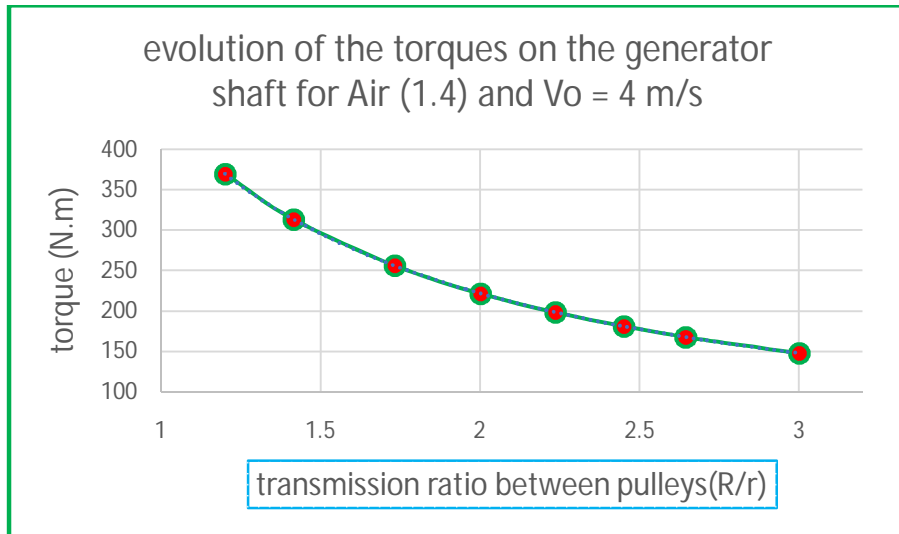


Fig. 5: Effect on generator torque as a function of the pulley ratio

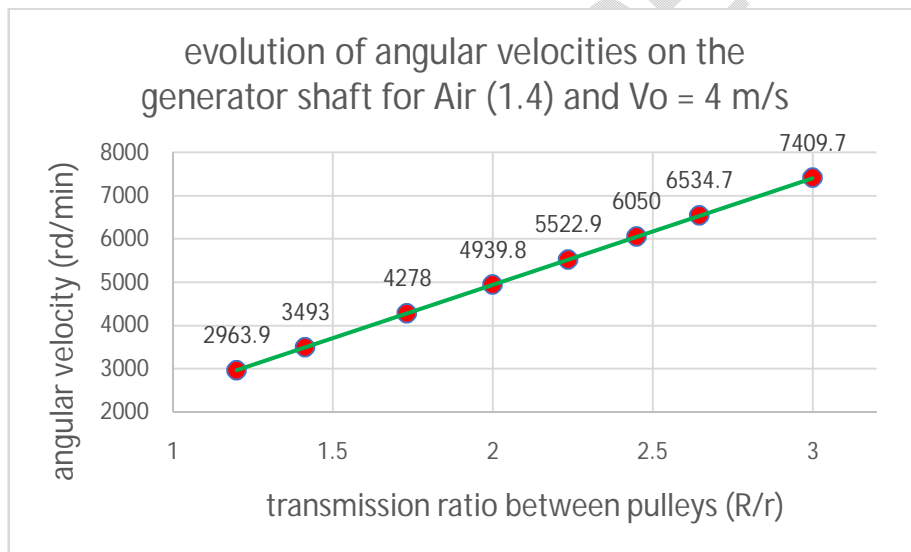


Fig. 6: Effect on the angular speed of the generator as a function of the pulley transmission ratio

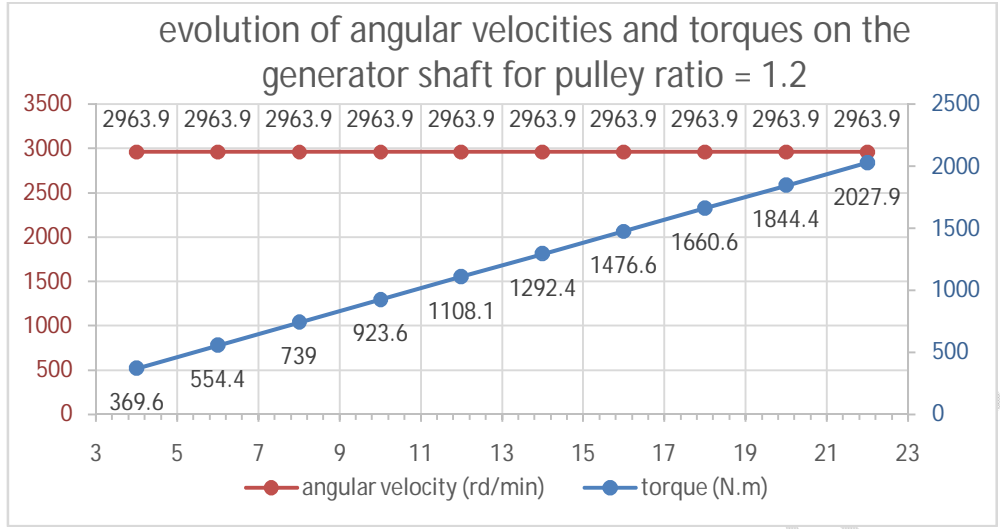


Fig. 7: Effect on torque and angular velocity as a function of speed at the convergent inlet

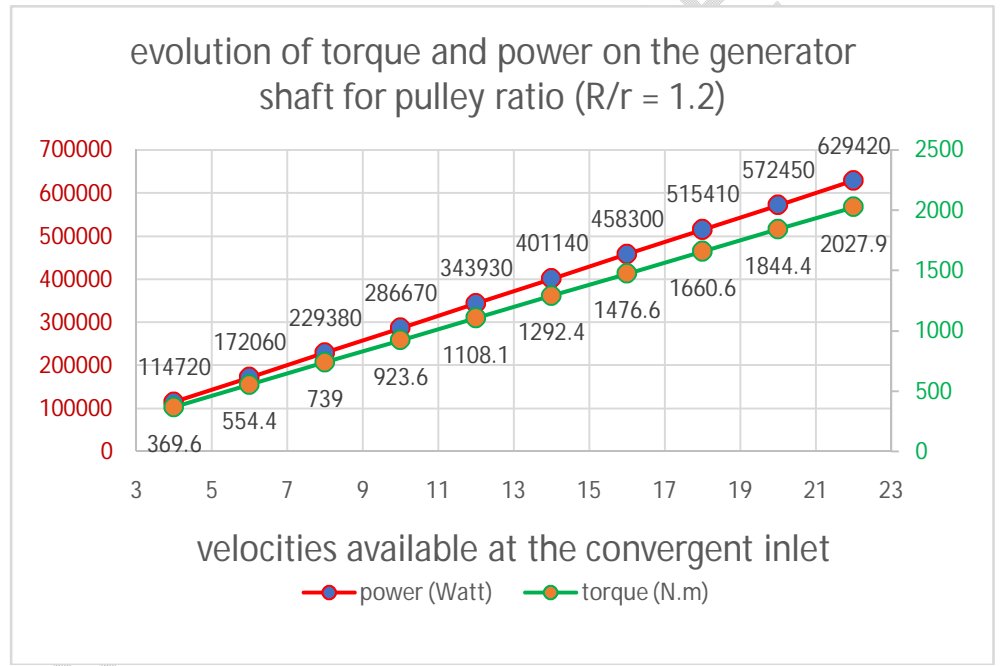


Fig. 8: Effect on torque and power as a function of speed at the convergent inlet

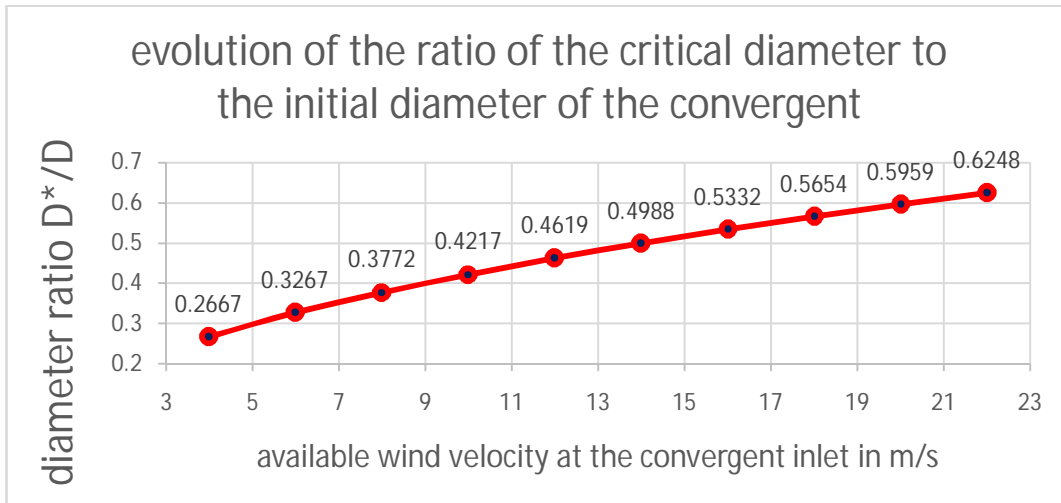


Fig. 9: Variation of the ratio of the critical diameter to any diameter for velocities at the convergent inlet.

Another numerical simulation from Matlab program shows that the values of the mechanical characteristics of an electric generator can be obtained for a given gas. By replacing (γ) with its value for different gases, it was possible to recover the expected angular velocity, torque, and power on the axis of an electric generator.

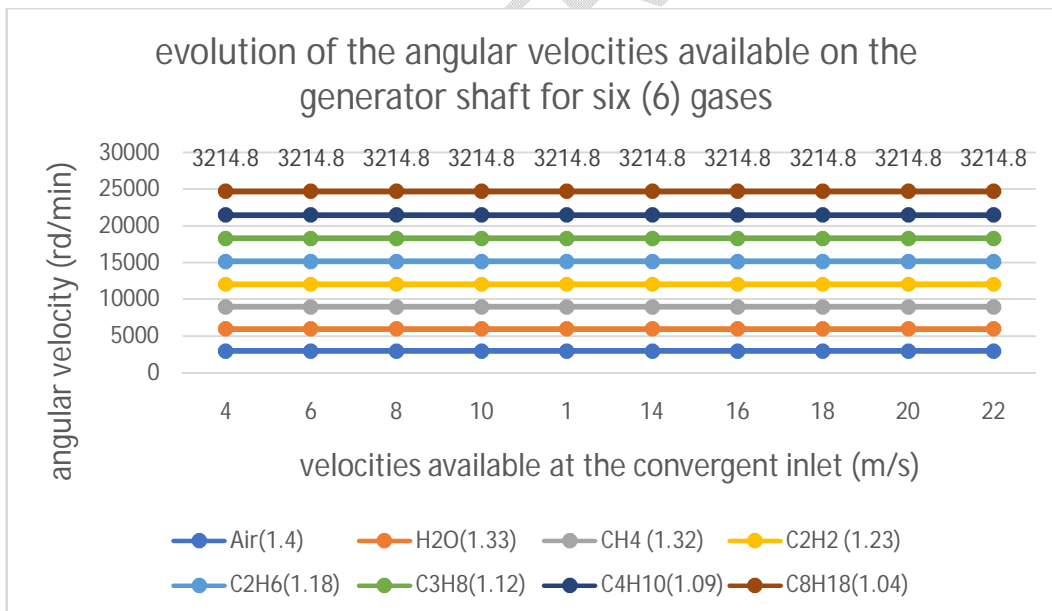


Fig. 10: Classification of angular velocities on the generator shaft for different gases according to the speed available at the convergent inlet

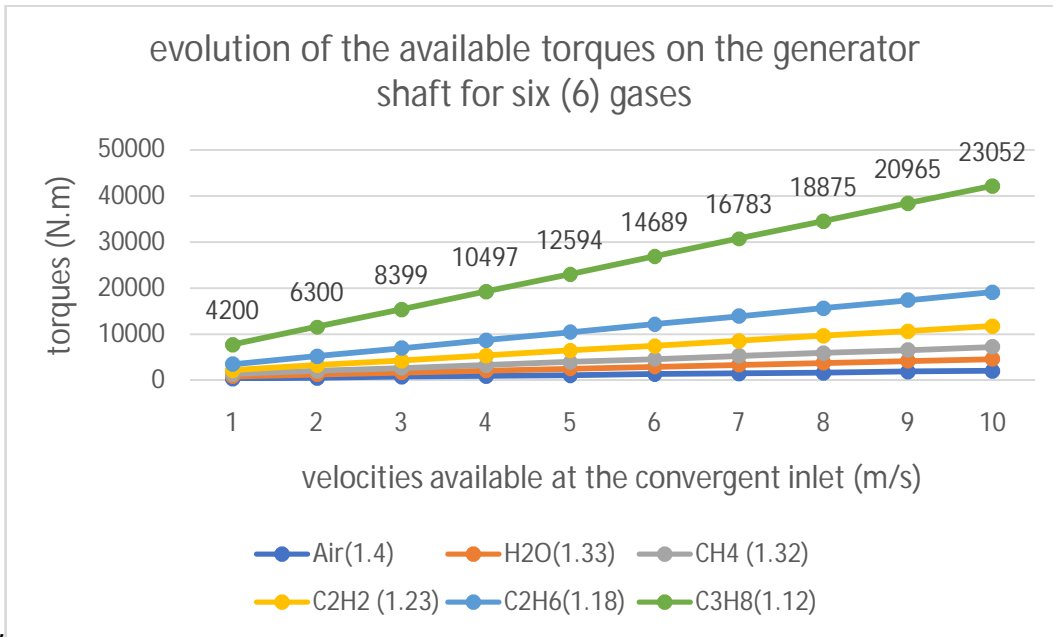


Fig. 11: Classification of the torques on the generator shaft for different gases according to the speed available at the convergent inlet.

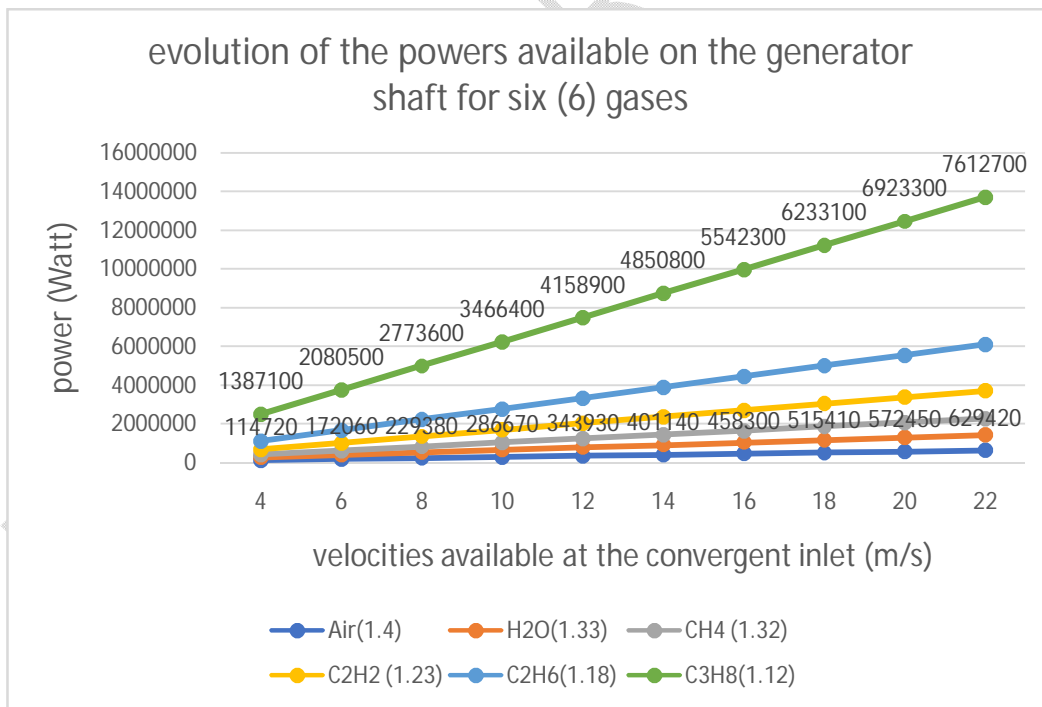


Fig. 12: Classification of the powers of the generator shaft for different gases according to the speed available at the convergent inlet.

Fig. 5 and Fig. 6 show that the torque on the shaft decreases with the transmission ratio while the angular speed increases. As for Fig. 7, it shows that for a given ratio, the angular

speed remains constant and that the torque increases with the speed of the convergent inlet. On the other hand, Fig. 8 shows that torque and power increase with the wind speed at the convergent inlet. The evolution of Fig. 9 shows a continuous increase in the ratio of the diameters of the speeds available at the entrance of the convergent. This means that the device will be very bulky when the installation of high-power plants is considered. However, this space requirement will be of a completely different nature. It will be horizontal against the verticality of the traditional wind turbines.

As for Fig. 10, it had already been shown (see Fig. 7) that the angular velocity of the generator shaft does not depend on the wind speed available at the convergent inlet, but only on the transmission ratio of the pulleys. Therefore, the horizontal aspect of the curves is well justified. On the other hand, what is interesting to observe in Fig. 10 is the stratification of the different curves. It can be seen that the lower (γ), the higher the speed collected on the shaft.

Two observations can be noted on Fig. 11: on the one hand, the torque on the generator shaft increases with the available wind speed at the convergent inlet. On the other hand, for the same wind speed at the convergent inlet, the torque is higher when (γ) is low. More concretely, Air ($\gamma=1.4$) would produce the same wind speed, a lower torque on the generator shaft than by ethane ($\gamma=1.18$) in the same condition.

From all that has just been shown, there is no longer any doubt that the powers collected on the generator shaft should be based on the same logic, i.e., the more (γ) is low, the higher the power released. This is what Fig. 12 shows. If, for example, there is a source of production of methane, or a deposit of this gas, it would be possible, by its implementation, to actuate a generator much more powerful than if it were aired, thus a production of electric energy much greater.

With these observations, it appears that it is now possible to make a given generator turn at its operating point. It will suffice to realize the speed of the operating point by a judicious choice of the transmission ratio by referring to equation (6), all things being equal.

The results obtained can be related to the work of other researchers. Indeed, Elbatran et al. [25] proposed six new ducted nozzle systems to increase rotor efficiency. Their results showed that the new designs helped to increase the velocity, increase the pressure difference to allow more flows to pass through the turbine, reduce the negative torque of the return blade, and finally improve the extracted power. The results of Mohammadi et al. [26] showed a complete agreement with the results of Elbatran et al. [25] with a power extraction three times higher than the conventional rotor without nozzle. We can also highlight the results of Chen et al. [27], who studied the effect of wind deflectors on a parallel matrix system of Savonius rotors. Their results showed that the performance of the system was increased by 16% when the deflector system was used.

4. CONCLUSION

Wind turbines are a valuable source for small-and large-scale power generation today. Low efficiency, negative static torque and self-starting problems are some of the problems faced by different types of turbines. Power augmentation devices have shown an effective solution to overcome these drawbacks.

This study attempts to analyze the effect of a flux convergent on an experimental wind device in terms of angular velocity, torque, and power output. The main findings are as follows:

- i. The air convergent (with different input and output sections) used on the device increases the output speed by around ten times the input speed [10].
- ii. The torque on the generator shaft decreases with the transmission ratio while the angular velocity increases.
- iii. The angular velocity on the generator shaft does not depend on the wind speed available at the convergent input, but only on the transmission ratio of the pulleys.
- iv. The torque on the generator axis increases with the wind speed available at the convergent inlet. For the same gas velocity at the convergent inlet, the torque is higher when (γ) is low. Also, the lower (γ) the higher the power output.
- v. The device can be trimmed to the power to be delivered by the generator. The wind speed through the fan flow being known, it is then necessary to define the dimensions of the convergent by the choice of its small section and the calculation of the large one [10]. Then, the transmission ratio of the pulleys must be chosen to obtain the speed of the operating point, and everything is done.

REFERENCES

1. Tong W. Wind power generation and wind turbine design. WIT press. Ashurst. 2010.
2. Abdel-Aziz M, Abdel-Aziz F. Hybrid Nanocrystal Photovoltaic/Wind Turbine Power Generation System in Buildings. *Journal of Advanced Research in Materials Science*.2018; 40: 8–19.
3. Eriksson S, Bernhoff H, Leijon M. Evaluation of different turbine concepts for wind power. *Renewable and Sustainable Energy Reviews*.2008; vol. 12, pp. 1419–1434.
4. Johari M, Jalil M, Shariff M. Comparison of horizontal axis wind turbine (HAWT) and vertical axis wind turbine (VAWT). *International Journal of Engineering and Technology*.2018; vol. 7, pp. 74–80.
5. Pope K, Dincer I, Naterer G. Energy and exergy efficiency comparison of horizontal and vertical axis wind turbines. *Renewable energy*.2010; vol. 35, pp. 2102–2113.
6. Bhutta M, Hayat N. Farooq A, Ali Z, Jamil S, and Hussain Z. Vertical axis wind turbine—A review of various configurations and design techniques. *Renewable and Sustainable Energy Reviews*.2012; vol. 16, pp. 1926–1939.
7. Kumar R, Raahemifar K, and Fung A. A critical review of vertical axis wind turbines for urban applications. *Renewable and Sustainable Energy Reviews*.2018; vol. 89, pp. 281–291.
8. Dragomirescu A. Performance assessment of a small wind turbine with crossflow runner by numerical simulations. *Renewable Energy*.2011; 36, pp. 957 – 965.
9. Chong WT, Shiah Y, Wong KH, Sukiman NL, Poh SC, Wang CT. Performance enhancements on vertical axis wind turbines using flow augmentation systems: A review. *Renewable and Sustainable Energy Reviews*.2017; 73, pp. 904–921.
10. Guero M, PRODJINONTO V. Design and Analysis of An Innovative Wind Flow Accelerator for Wind Devices. *International Journal of Progressive Sciences and Technologies*.2022; 32(2), 350–358.
11. Shigemitsu T, Fukutomi J, Toyohara M. Performance and flow condition of cross-flow wind turbine with a symmetrical casing having side boards. *International Journal of Fluid Machinery and System*.2016; 9, pp. 169–174.

12. Takao M, Maeda T and Kamada Y. A Straight-blades Vertical Axis Wind Turbine with a Directed Guide Vane Row. *Journal of Fluid Science and Technology*.2008; 3, pp. 379–386.
13. Chong WT, Poh SC, Fazlizan A, Pan KC. Vertical axis wind turbine with omnidirectional guide vane for urban high-rise building. *Journal of Central South University*.2012; 19, pp. 727–732.
14. Korprasertsak N and Leephakpreeda T. Analysis and optimal design of wind boosters for Vertical Axis wind Turbines at low wind speed. *Journal of Wind Engineering and Industrial Aerodynamics*.2016; 159, pp. 9–18.
15. K. Lee, S. Tsao, C. Tzeng, and H. Lin, “Influence of the vertical wind and wind direction on the power output of a small vertical-axis wind turbine installed on the rooftop of a building,” *Applied Energy*, vol. 209, pp. 383–391, 2018.
16. Gumilar L, Kusumawardana A, Habibi M, Afandi A, Prihanto D, and Aji A. Performance analysis of vertical wind turbine type Savonius-I based on wind speed, rotation speed, and number of blades. In 2019 International Seminar on Application for Technology of Information and Communication (iSemantic).2019; pp. 383–388.
17. Rezaeiha A, Kalkman I, and Blocken B. Effect of pitch angle on power performance and aerodynamics of a vertical axis wind turbine. *Applied energy*.2017; vol. 197, pp. 132–150.
18. Mantravadi B, Sriram K, Mohammad A, Vaitla L, and Velamati R. Effect of solidity and airfoil on the performance of vertical axis wind turbine under fluctuating wind conditions. *International Journal of Green Energy*.2019; vol. 16, pp. 1329–1342.
19. Sun X, Zhu J, Hanif A, Li Z, and Sun G. Effects of blade shape and its corresponding moment of inertia on self-starting and power extraction performance of the novel bowl-shaped floating straight-bladed vertical axis wind turbine. *Sustainable Energy Technologies and Assessments*.2020; vol. 38, p. 1–18.
20. Zamani M, Nazari S, Moshizi S, and Maghrebi M. Three-dimensional simulation of J-shaped Darrieus vertical axis wind turbine. *Energy*.2016; vol. 116, pp. 1243–1255.
21. Hameed M, Afaq S, and Shahid F. Finite element analysis of a composite VAWT blade. *Ocean Engineering*.2015; vol. 109, pp. 669–676.
22. Wang L, Kolios A, Nishino T, Delafin P, and Bird T. Structural optimization of vertical-axis wind turbine composite blades based on finite element analysis and genetic algorithm. *Composite Structures*.2016; vol. 153, pp. 123–138.
23. Chong W, Muzammil W, Wong K, Wang C, Gwani M, Chu Y and al. Cross axis wind turbine: Pushing the limit of wind turbine technology with complementary design. *Applied Energy*.2017; vol. 207, pp. 78–95.
24. Alom N and Saha U. Four decades of research into the augmentation techniques of Savonius wind turbine rotor. *Journal of Energy Resources Technology*.2018; vol. 140.
25. Elbatran AH, Yasser MA, and Shehata AS. Performance study of ducted nozzle Savonius water turbine, comparison with conventional Savonius turbine. *Energy*.2017;134: 566–584.
26. Mohammadi M, Mohammadi R, Ramadan A, and Mohamed MH. Numerical investigation of performance refinement of a drag wind rotor using flow augmentation and momentum exchange optimization. *Energy*. 2018;158: 592–606.
27. Chang-An C, Tien-Yang H, and Chiun-Hsun C. Novel plant development of a parallel matrix system of Savonius wind rotors with wind deflector. *Journal of Renewable and Sustainable Energy*. 2015;7(1):31–35.